Journal of Solid State Chemistry 183 (2010) 1055–1062

Contents lists available at ScienceDirect

Journal of Solid State Chemistry

journal homepage: www.elsevier.com/locate/jssc

Structure investigation of fluorinated aluminophosphate ULM-3 Al templated by 3-methylaminopropylamine

Natasa Zabukovec Logar [a,d,*], Gregor Mali [a], Nevenka Rajic [b], Sanja Jevtic [b], Mojca Rangus [a], Amalija Golobic [c], Venceslav Kaucic [b]

[a] National institute of Chemistry, Hajdrihova 19, 1000 Ljubljana, Slovenia
[b] Faculty of Technology and Metallurgy, University of Belgrade, Karnegijeva 4, 11000 Belgrade, Serbia
[c] Faculty of Chemistry and Chemical Technology, University of Ljubljana, Askerceva 5, 1000 Ljubljana, Slovenia
[d] University of Nova Gorica, Pristava, Kostanjeviska 16, 5000 Nova Gorica, Slovenia

ARTICLE INFO

Article history:
Received 29 October 2009
Received in revised form
19 February 2010
Accepted 28 February 2010
Available online 12 March 2010

Keywords:
Aluminophosphate
Microporous material
ULM-3
3-Methylaminopropylamine
Single-crystal structure analysis
Fluoride medium

ABSTRACT

A single-crystal X-ray diffraction analysis of an open-framework aluminophosphate ULM-3 Al prepared by 3-methylaminopropylamine (MAPA) as structure-directing agent revealed an orthorhombic *Pcab* symmetry ($a=9.9949(4)$ Å, $b=15.8229(7)$ Å, $c=18.1963(5)$ Å, $R=0.0648$, $Z=8$, unit cell formula $[Al_{24}P_{24}O_{96}F_{16}\cdot C_{32}H_{112}N_{16}]$), which differs from the $Pbc2_1$ symmetry of the structural analogue prepared in the presence of 1,4-diaminobutane. The ^{27}Al, ^{31}P, ^{19}F, ^{13}C and ^{1}H NMR investigations, which were performed to study in detail MAPA arrangement inside the framework as well as the interactions of MAPA with the aluminophosphate host, confirmed the crystal symmetry and the proposed hydrogen bonding scheme between the template and the framework.

1. Introduction

Porous aluminophosphates are still a fertile field of investigations because their structures can be tailored with regard to the shape, size and dimensionality of channels and cages within the frameworks. The method widely used in the synthesis of these materials includes the use of organics (such as amines or quaternary ammonium ions), which act as structure-directing agents, assisting in the organization of building blocks to arrange themselves in an open-framework host/guest structure. There is strong evidence that some organics exhibit specific structure-directing role in the formation of a certain type of channels. As an example, *n*-diaminopropane directs the formation of one-dimensional channel system into several different aluminophosphate topologies [1,2].

Recently, we investigated the structure-directing role of 3-methylaminopropylamine (MAPA) in the synthesis of porous structures. We prepared a novel layered zinc phosphate [3,4] and an open-framework $AlPO_4$-21 [5]. Since it is a well-known fact that the presence of fluoride ions in an aluminophosphate reaction mixture can lead to novel structures [6–26], we carried out the experiments with MAPA also in a fluoride medium. In fluorinated aluminophosphate structures, the fluorine atoms usually bridge aluminum building units and typically occupy one or two vertices of the aluminum octahedra [7]. By using MAPA in a fluoride medium, we obtained a fluorinated aluminophosphate (ULM-3 Al-MAPA), whose structure was analogous to aluminophosphate ULM-3 Al [26] and gallophosphate ULM-3 structures [27,28], which were prepared by using symmetric diamines as structure-directing agents.

We report here on the structure analysis of ULM-3 Al-MAPA by the use of single crystal X-ray diffraction and NMR spectroscopy. Beside the two structures that we prepared [3–5], the literature review revealed only two other structures where MAPA had been used as a template in the synthesis, i.e. two layered aluminophosphates denoted MDAP-1 and MDAP-3 [29,30]. The third reported structure MDAP-2 was isostructural with $AlPO_4$-21 [29].

2. Experimental

2.1. Synthesis and materials

ULM-3 Al-MAPA was synthesized hydrothermally under autogenous pressure using hydrated Al_2O_3 (77.8 wt%, Aldrich), orthophosphoric acid (85 wt%, Aldrich), 3-methylaminopropylamine (98 wt%, Fluka), HF (40 wt%, Merck) and H_2O following the

* Corresponding author at: National institute of Chemistry, Hajdrihova 19, 1000 Ljubljana, Slovenia.
E-mail address: natasa.zabukovec@ki.si (N. Zabukovec Logar).

0022-4596/$ - see front matter © 2010 Elsevier Inc. All rights reserved.
doi:10.1016/j.jssc.2010.02.020

molar ratios $0.5Al_2O_3$:H_3PO_4:0.5MAPA:HF:$100H_2O$. To a finely dispersed water suspension of Al_2O_3, phosphoric acid, MAPA and HF were successively added drop wise. The mixture was homogenized using ULTRA TURRAX®, IKA® T18 basic stirrer. Crystallization was performed in a Teflon-lined stainless steel autoclave at 160 °C for 1–7 days. The white powder product was filtered off, washed with dematerialized water, and was dried at 60 °C overnight. Elemental analysis gave the following stoichiometry: $(AlPO_4)_3F_2(C_4H_{14}N_2)$.

Large colorless ULM-3 Al-MAPA crystals up to 200 μm were obtained from the reaction mixture which contained cobalt(II) ions. The cobalt acetate and aluminum oxide were used in a molar ratio 1:4, respectively, since transition metal acetates give the best results regarding the phase purity, crystallinity and crystal quality of aluminophosphates and their metal-containing analogues. The reaction mixture yielded the product mainly consisting of large colorless prismatic crystals that were sprinkled by blue spots in some places. The blue impurities were removed by decantation after the product was treated ultrasonically. Elemental analysis of the colorless crystals yielded the same stoichiometry as was that obtained for the white powder product.

2.2. Instrumentation

The size and the morphology of the crystals in the samples were studied by scanning electron microscope SUPRA 35 VP (Carl Zeiss). The qualitative analyses of the collected XRPD patterns were performed using the Crystallographica Search-Match programs [31].

A colorless prismatic single crystal ($0.20 \times 0.10 \times 0.05\ mm^3$) of ULM-3 AL-MAPA was selected for the X-ray single-crystal structure analysis. The room-temperature intensity data were collected on a Nonius Kappa CCD diffractometer by using the Mo*K*α radiation. Unit cell parameters were determined by least-square refinement on the basis of 1633 reflections. The structure was solved combining the SHELXS and Fourier maps calculation using the SHELXL-97 [32]. The later was also used for the structure refinement and the interpretation. Further details of the data collection and reduction are contained in Table 1. Final atomic parameters of all atoms for the ULM-3 Al-MAPA structure are listed in Table 2, selected bond distances in Table 3 and selected bond angles in Table 4. The framework atoms were refined anisotropically. The extra-framework non-hydrogen atoms were refined isotropically. H atoms on template molecules were included in calculated positions. N2 atom in the template molecule is disordered over two sites, whose occupancies were constrained to the sum of 1.0. Attempts to refine the structure in the lower symmetry did not remove the disorder of N atoms. ATOMS [33] and Ortep [34] programs were used for the drawings of the structure. The supplementary crystallographic data for this paper (CCDC 752518) can be obtained free of charge from The Cambridge Crystallographic Data Centre via ⟨www.ccdc.cam.ac.uk/data_request/cif⟩.

NMR spectra were recorded on a 600 MHz (14.1 T) Varian VNMRS spectrometer using a Varian 3.2 mm double resonance MAS probe for standard single pulse, spin echo and cross-polarization (CP) MAS experiments, and a 5 mm Doty triple resonance Supersonic Spinning Probe for 2D Heteronuclear Chemical-Shift Correlation (HETCOR) experiments. Sample was spun at 12.5 kHz under the magic angle during all measurements, except during ^1H spectroscopy, where the spinning rate was 20 kHz. ^{27}Al, ^{31}P and ^{19}F MAS spectra were recorded with a

Table 1
Experimental conditions and crystallographic data for the single X-ray diffraction study of ULM-3 Al-MAPA.

Formula of asymmetric unit	$C_4H_{14}Al_3F_2N_2O_{12}P_3$
Formula weight	494.02
Crystal color, habit	Colorless, prismatic
Crystal system	Orthorhombic
a (Å)	9.9949(4)
b (Å)	15.8229(7)
c (Å)	18.1963(5)
V (Å^3)	2877.7(2)
Z	8
Space group	*Pcab*
D_C (mg m^{-3})	2.281
hkl data limits	$-9 \le h \le 9,\ -15 \le k \le 15,\ -17 \le l \le 17$
$2\theta_{max}$ (deg.)	40.74
R_{int}	0.0381
μ(Mo*K*α) (mm^{-1})	6.96
λ(Mo*K*α) (Å)	0.71073
T(K)	293(2)
Absorption correction	none
Total data	1404
Observed data ($F^2 \ge 2\sigma(F^2)$)	1092
Parameters	206
R (on F^2)	0.066
R_w (on F^2)	0.172
$\Delta\rho_{max}$ (eÅ^{-3})	0.819
$\Delta\rho_{min}$ (eÅ^{-3})	−0.739

Table 2
Fractional atomic coordinates and equivalent displacement parameters (Å^2); $U_{eq} = (1/3)\ \Sigma_i\Sigma_j U_{ij} a_i^* a_j^* a_i a_j$.

	x	*y*	*z*	U_{eq}/U_{iso}	Part. occ.
Al1	−0.3153(4)	1.0375(3)	0.2823(2)	0.0110(12)	
Al2	−0.1690(4)	0.8501(3)	0.3234(2)	0.0110(12)	
Al3	−0.3423(4)	1.0097(3)	0.0940(2)	0.0107(12)	
P1	−0.1407(4)	1.0093(2)	0.42271(19)	0.0119(11)	
P2	−0.3542(4)	1.1836(2)	0.16993(19)	0.0125(11)	
P3	−0.1159(4)	0.9427(2)	0.18548(19)	0.0126(11)	
F1	−0.3213(8)	0.9210(5)	0.3072(4)	0.019(2)	
F2	−0.3995(8)	1.0039(5)	0.1953(4)	0.016(2)	
O1	−0.4954(9)	0.9581(6)	0.0726(5)	0.015(2)	
O2	−0.2907(9)	1.0191(6)	−0.0025(5)	0.015(2)	
O3	−0.1363(9)	0.9160(6)	0.3998(5)	0.016(2)	
O4	−0.2176(9)	1.0636(6)	0.3670(5)	0.012(2)	
O5	−0.2708(10)	0.7629(6)	0.3451(5)	0.017(2)	
O6	−0.3160(9)	1.1485(5)	0.2461(5)	0.015(2)	
O7	−0.3169(10)	1.1200(6)	0.1078(5)	0.018(2)	
O8	−0.0023(9)	0.7926(6)	0.3350(5)	0.014(2)	
O9	−0.2022(9)	0.9433(6)	0.1152(5)	0.016(2)	
O10	−0.1412(9)	0.8572(6)	0.2254(4)	0.014(2)	
O11	−0.1534(9)	1.0162(6)	0.2351(5)	0.015(2)	
O12	−0.4689(9)	1.0518(6)	0.3365(5)	0.012(2)	
N1	−0.0250(13)	1.1776(8)	0.3039(7)	0.029(3)	
H1	0.0069	1.1284	0.2880	0.11(3)	
H2	−0.0354	1.2125	0.2659	0.11(3)	
H3	−0.1036	1.1694	0.3257	0.11(3)	
C1	0.0704(18)	1.2153(11)	0.3573(9)	0.038(5)	
H4	0.1383	1.1737	0.3692	0.11(3)	
H5	0.1148	1.2630	0.3343	0.11(3)	
C2	0.0074(17)	1.2436(11)	0.4251(8)	0.035(4)	
H6	−0.0342	1.1963	0.4502	0.11(3)	
H7	−0.0609	1.2854	0.4145	0.11(3)	
C3	0.1174(18)	1.2824(11)	0.4733(9)	0.036(4)	
H8	0.1812	1.2384	0.4856	0.11(3)	
H9	0.1645	1.3247	0.4447	0.11(3)	
N2A	0.0695(19)	1.3232(12)	0.5443(10)	0.027(7)	0.66(3)
H10A	0.0335	1.2827	0.5729	0.11(3)	0.66(3)
H11A	0.1410	1.3442	0.5681	0.11(3)	0.66(3)
N2B	0.074(4)	1.369(2)	0.486(2)	0.030(14)	0.34(3)
H12B	0.1468	1.3979	0.4994	0.11(3)	0.34(3)
H13B	0.0487	1.3891	0.4418	0.11(3)	0.34(3)
C4	−0.0280(19)	1.3902(12)	0.5356(10)	0.045(5)	
H14	−0.0686	1.3862	0.4880	0.11(3)	
H15	0.0157	1.4440	0.5404	0.11(3)	
H16	−0.0956	1.3850	0.5728	0.11(3)	

Table 3
Selected bond distances (Å).

Al1–O12	1.839(9)
Al1–O11	1.863(10)
Al1–F2	1.869(8)
Al1–O4	1.872(9)
Al1–O6	1.876(9)
Al1–F1	1.898(8)
Al2–O5	1.758(10)
Al2–O3	1.768(9)
Al2–O10	1.810(9)
Al2–O8	1.910(10)
Al2–F1	1.914(9)
Al3–O1	1.777(10)
Al3–O7	1.782(10)
Al3–O9	1.793(10)
Al3–O2	1.835(9)
Al3–F2	1.932(8)
P1–O2	1.532(10)
P1–O3	1.535(10)
P1–O4	1.535(9)
P1–O1	1.544(10)
P2–O8	1.530(10)
P2–O5	1.531(10)
P2–O6	1.541(10)
P2–O7	1.558(10)
P3–O11	1.520(10)
P3–O12	1.525(10)
P3–O9	1.543(10)
P3–O10	1.555(10)
N1–C1	1.49(2)
C1–C2	1.46(2)
C2–C3	1.54(2)
C3–N2A	1.52(2)
N2A–C4	1.45(3)
C3–N2B	1.46(3)
N2B–C4	1.40(3)

standard single pulse sequence with repetition delays of 0.5, 30 and 5 s and the number of scans accumulated were 6500, 140 and 16, respectively. ^{1}H spectrum was measured with the spin echo MAS sequence with 16 accumulated scans and 5 s repetition delay. ^{1}H–^{13}C CP MAS spectra were recorded with 5 s repetition time and 14,000 accumulations. The chemical shift axis for aluminum was referenced to 1 mol dm^{-3} $Al(NO_3)_3$, for phosphorus to 85 wt% H_3PO_4, to $CFCl_3$ for fluorine spectrum and to TMS for ^{1}H and ^{13}C. The HETCOR spectra were recorded with the hypercomplex approach. In ^{27}Al–^{31}P HETCOR experiment 50 steps were taken along the indirect dimension and 1600 scans were accumulated per step. For the ^{27}Al–^{19}F HETCOR experiment the number of steps in the indirect dimension was 100 and the number of scans was 2000. Repetition delay in both experiments was 0.1 s.

3. Results and discussion

Crystallization of cobalt(II)-free reaction mixture gave the white powder product. SEM analysis revealed that it contains ball aggregates. Cobalt(II)-contained reaction mixture provided large colorless crystals with a prismatic morphology. Both products are shown in Fig. 1. X-ray powder diffraction patterns confirmed the structure analogy with the open-framework ULM-3 Al [26] and ULM-3 [27] structures.

3.1. Single-crystal X-ray diffraction analysis

Single-crystal X-ray structure analysis showed that ULM-3 Al-MAPA crystallizes in an orthorhombic space group *Pcab* with lattice parameters $a=9.9949(4)$, $b=15.8229(7)$ and $c=18.1963(5)$ Å.

Table 4
Selected bond angles (deg.).

O12–Al1–O11	174.2(5)
O12–Al1–F2	96.5(4)
O11–Al1–F2	87.1(4)
O12–Al1–O4	88.1(4)
O11–Al1–O4	88.1(4)
F2–Al1–O4	174.4(4)
O12–Al1–O6	94.0(4)
O11–Al1–O6	90.6(4)
F2–Al1–O6	88.1(4)
O4–Al1–O6	94.8(4)
O12–Al1–F1	88.0(4)
O11–Al1–F1	87.8(4)
F2–Al1–F1	85.0(4)
O4–Al1–F1	92.0(4)
O6–Al1–F1	173.0(4)
O5–Al2–O3	113.2(5)
O5–Al2–O10	111.0(5)
O3–Al2–O10	135.2(5)
O5–Al2–O8	96.1(5)
O3–Al2–O8	91.9(4)
O10–Al2–O8	90.2(4)
O5–Al2–F1	92.0(4)
O3–Al2–F1	85.5(4)
O10–Al2–F1	86.2(4)
O8–Al2–F1	171.9(4)
O1–Al3–O7	127.1(5)
O1–Al3–O9	116.8(5)
O7–Al3–O9	115.6(5)
O1–Al3–O2	94.0(4)
O7–Al3–O2	90.9(4)
O9–Al3–O2	91.9(4)
O1–Al3–F2	86.1(4)
O7–Al3–F2	87.3(4)
O9–Al3–F2	89.9(4)
O2–Al3–F2	177.9(4)
O2–P1–O3	110.6(5)
O2–P1–O4	107.8(5)
O3–P1–O4	112.0(5)
O2–P1–O1	109.8(5)
O3–P1–O1	108.0(5)
O4–P1–O1	108.7(5)
O8–P2–O5	108.3(5)
O8–P2–O6	112.4(5)
O5–P2–O6	108.8(5)
O8–P2–O7	110.4(5)
O5–P2–O7	105.7(5)
O6–P2–O7	111.1(5)
O11–P3–O12	110.5(5)
O11–P3–O9	110.5(5)
O12–P3–O9	108.7(5)
O11–P3–O10	110.4(5)
O12–P3–O10	109.2(5)
O9–P3–O10	107.6(5)

The framework is built up of hexanuclear units formed by three PO_4 tetrahedra, two AlO_4F trigonal bipyramids and one AlO_4F_2 octahedra. The three-dimensional negatively charged framework has characteristic 10-membered ring channels running along [1 0 0], which are interconnected with the 8-membered ring channels running along [1 0 1] and [1 0 −1] directions (Fig. 2). The doubly protonated template molecules, which are located in the 10-membered ring channels compensate for the negative charge of the framework. The lower symmetry of the ULM-3 Al analogue, which was reported to be due to ordered sub-network of the symmetric 1,4-diaminobutane molecules, was not observed here.

There are three crystallographically distinct phosphorous sites and three aluminum sites in the asymmetric unit (Fig. 3). All P atoms are tetrahedrally coordinated and share four oxygen atoms with the adjacent Al atoms. The P–O bond lengths in PO_4 tetrahedra are in the range from 1.520(10) to 1.558(10) Å (Table 3) and the O–P–O bond angles from 107.6(5)° to 112.4(6)° (Table 4). The Al–O/F bond lengths in AlO_4F trigonal

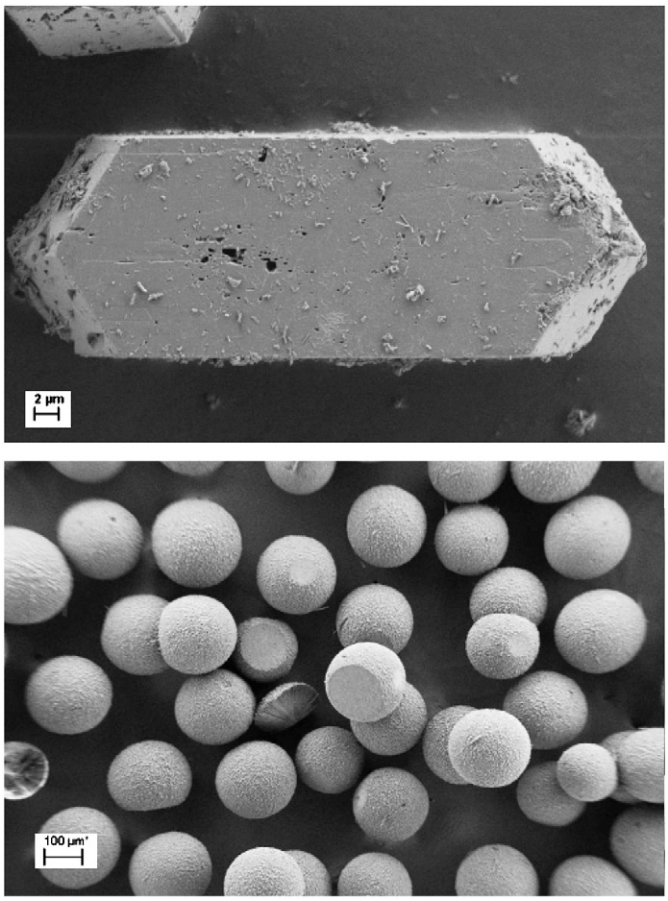

Fig. 1. SEM pictures of ULM-3 Al-MAPA single-crystal and powder.

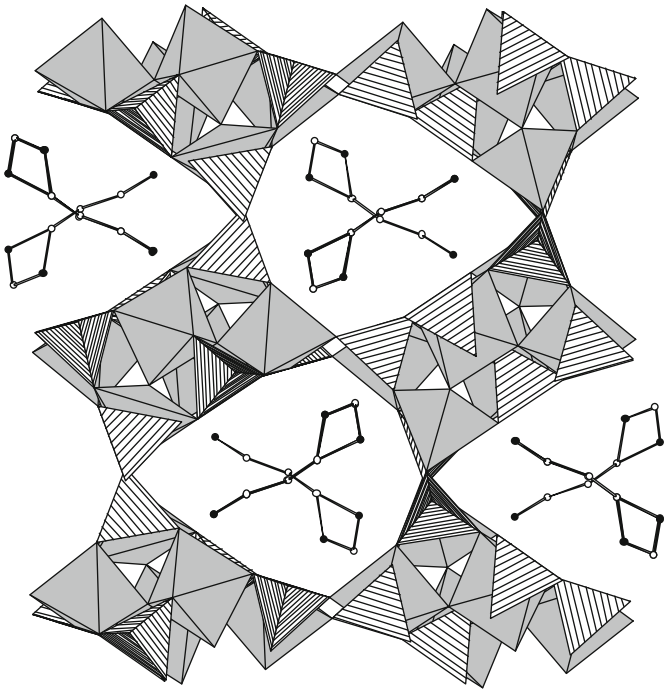

Fig. 2. Polyhedral presentation of ULM-3 Al-MAPA framework with extra-framework 3-methylaminopropylamine species (Al-polyhedra=grey, PO_4=lined, C atoms=white circles, N atoms=black circles).

bipyramids range from 1.839(9) to 1.898(8) Å and Al–O/F bond lengths in AlO_4F_2 octahedra range from 1.758(10) to 1.932(8) Å, as shown in Tables 3 and 4. The values are comparable with those in similar structures [25]. The N2 atom in the template molecule is disordered over two positions N2A and N2B, which are 1.121(1) Å apart. The occupancies of N2A and N2B sites refined to 0.66(3):0.34(3). This disorder could be due to fact that both positions have a surrounding that enable stabilization of the structure by intermolecular N–H…O hydrogen bonding through both hydrogen atoms of the N2 amino group. The N2A atom form H-bonds with O7 and O8 atoms with bond distances 2.87(2) and 2.94(2) Å, respectively. The N2B atom donates H-bonds to different framework O2 and O12 atoms, i.e. N2B–O2 distance is 2.81(2) Å and N2B–O12 distance 3.03(2) Å. The well-ordered N1 atom is a donor of bifurcated hydrogen bonds through all three hydrogen atoms. All but one, with the N1…O12 contact distance 2.877(16), are weak. The details on hydrogen bonding geometry are reported in Table 5. Interestingly there are only weak N–F contacts, i.e. from 3.13(2) to 3.27(2) Å.

MAPA in $AlPO_4$-21 was, for comparison, statistically disordered mainly due to its asymmetry and to space confinements in the $AlPO_4$-21 framework. It could be mentioned that a disorder on one N atom in linear diamine template molecules, 1,4-diaminobutane and 1,5-diaminopentane, was also observed in the gallophosphate ULM-3 structure and was assigned to the lack of H-bonds of this N atoms with the framework, i.e. to the conformational freedom of the template. Such disorder was not observed in the ULM-3 Al structure.

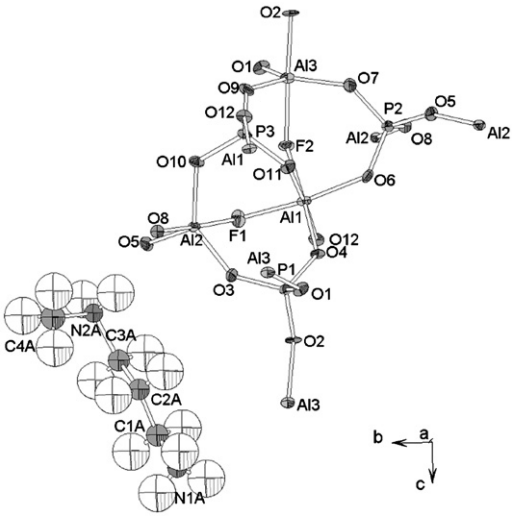

Fig. 3. Asymmetric unit of ULM-3 Al-MAPA with labeled atoms. The disorder of the template molecule is described in the text. Labels for all hydrogen atoms are omitted for clarity.

Table 5
Hydrogen bond contact distances D…A (Å) and D–H…A angles (deg.) in title compound, donor (D), acceptor (A).

N1–H1...O11	3.120(16)	120
N1–H1...F2 (1/2+x,2−y,1/2−z)	3.134(15)	153
N1–H2...O8 (x,1/2+y,1/2−z)	3.123(16)	164
N1–H2...O10 (x,1/2+y,1/2−z)	3.116(16)	124
N1–H3...O4	2.877(16)	137
N1–H3...O6	3.127(16)	120
N2A–H10A...O8 (−x,2−y,1−z)	2.94(2)	159
N2A–H11A...O7 (−x,5/2−y,1/2+z)	2.87(2)	170
N2B–H12B…O2 (−x,5/2−y,1/2+z)	2.81(4)	160
N2B–H13B…O12 (1/2+x,5/2−y,z)	3.03(4)	168

3.2. NMR study

A complementary view on the framework of aluminophosphate ULM-3 Al-MAPA can be obtained by ^{27}Al, ^{31}P and ^{19}F MAS NMR spectroscopy. One-dimensional spectra (Fig. 4) reveal three distinct aluminum, three distinct phosphorus and two distinct fluorine sites present in the asymmetric unit of this material, which confirms the selected *Pcab* symmetry of the structure. NMR study of ULM-3 Al analogue prepared in the presence of 1,4-diaminobultane revealed six distinct aluminum and six distinct phosphorus sites, which is consistent with the lower $Pbc2_1$ symmetry [35]. Observed isotropic shifts of aluminum resonances (see Table 6) confirm that among three aluminum sites one is hexa-coordinated and two are penta-coordinated. Two-dimensional ^{27}Al–^{19}F HETCOR NMR spectrum, furthermore, shows that both fluorine sites are bridging sites, connecting a hexa-coordinated Al atom with penta-coordinated ones (Fig. 5). Integrated intensities of all NMR signals match the proposed multiplicities of crystallographically inequivalent sites. All these NMR results are thus in nice agreement with results of single-crystal X-ray diffraction.

To carry out a more detailed analysis of the NMR spectra, we first note that the proposed crystal structure indicates that two AlO_4F trigonal bipyramids are not equally distorted. As a rough quantitative measure of a local distortion we can define a shear-strain parameter

$$|\Psi| = \Sigma_i \tan|\theta_i - \theta_0|, \quad (1)$$

which correlates well with the magnitude of quadrupolar coupling constant C_Q in case of tetrahedrally coordinated aluminum nuclei in aluminate sodalites, aluminosilicates and aluminophosphates [36], and in case of octahedrally coordinated titanium nuclei in perovskite and ilmenite $ATiO_3$ compounds [37]. In the former case angles θ_i were six O–Al–O bond angles for a given Al site and θ_0 was 109.5° of an undistorted tetrahedron. In the latter case angles θ_i were O–Ti–O bond angles for a given Ti site and θ_0 was 90° of an undistorted octahedron. In our case of trigonal bipyramids θ_0 is 120° when subtracted from 'in-plane' O–Al–O bond angles, and θ_0 is 90° when subtracted from O–Al–O and O–Al–F bond angles for bonds comprising the 'in-plane' oxygen atoms and either top-corner or bottom-corner oxygen or fluorine atom. Calculating shear strain for the two penta-coordinated aluminum sites allows us to assign the Al resonance at 24.8 ppm, exhibiting smaller quadrupolar coupling constant, to penta-coordinated Al3 site within the less distorted bipyramid, and the Al resonance at 23.2 ppm, exhibiting larger quadrupolar coupling constant, to penta-coordinated Al2 site within the more distorted bipyramid (for the values of shear-strain and quadrupolar-coupling parameters see Table 6). Because the correlation between shear strain and the magnitude of the quadrupolar coupling is not well tested for penta-coordinated aluminum sites, we also estimated quadrupolar-coupling constants by approximating anions surrounding Al sites with point charges. Such a crude approximation leads to the same assignment of penta-coordinated aluminum sites as the use of shear-strain parameter.

In the phosphorus NMR spectrum the completely resolved peak, resonating at −8 ppm, can be assigned to P3 site having two hexa-coordinated Al1 sites in its first cation coordination shell. Sites P1 and P2 are similar one to another and are both surrounded by only one hexa-coordinated and by three penta-coordinated aluminum sites. A tentative assignment of these two phosphorus sites to the two overlapping phosphorus resonances can be completed based on the correlation of the ^{31}P isotropic chemical shift and the mean P–O–Al bond angle [38–40]. This correlation between the experimentally determined NMR parameters and the structural data allows us to assign phosphorus NMR signal at −14.3 ppm to site P1 and phosphorus NMR signal at −15.4 ppm to site P2 (see Table 6). The proposed assignment can be verified with the help of ^{27}Al–^{31}P two-dimensional HETCOR NMR spectroscopy (Fig. 6), which provides an Al–P connectivity table. The derived connectivity table agrees with the proposed structure and proves that the assignment was correct. In an analogous way we can also use the ^{27}Al–^{19}F HETCOR spectrum and assign the two fluorine resonances to F1 and F2 sites and confirm that the measured NMR parameters nicely correlate with the structural data.

NMR spectroscopy also provided an insight into the arrangement of template 3-methylaminopropylamine molecules within the channels of the ULM-3 Al-MAPA crystals. ^{1}H MAS and ^{1}H–^{13}C CPMAS NMR spectra are shown in Fig. 7. In the former spectrum a strong contribution at about 7 ppm indicates that the MAPA are protonated within channels of ULM-3 Al-MAPA. The observed chemical shift is, namely, characteristic for protons within –(NH_2^+)– and –(NH_3^+) groups. A chemical shift of 7 ppm suggests that MAPA is bonded to the framework with relatively weak hydrogen bonds. In the spectrum of carbon nuclei we can clearly

Table 6
Isotropic chemical shift (δ_{CS}^{iso}) and quadrupolar (quadrupolar coupling constant C_Q and asymmetry η_Q) and shear-strain parameters ($|\Psi|$) for three aluminium sites of ULM-3 Al-MAPA. The values of δ_{CS}^{iso}, C_Q and η_Q were obtained by analyzing the experimental ^{27}Al MAS NMR spectrum using Dmfit [19]. For three phosphorus sites isotropical chemical shifts are related to mean P–O–Al bond angles θ_{P-O-Al}.

	δ_{CS}^{iso} (ppm)	C_Q (MHz)	η_Q	$\|\Psi\|$		δ_{CS}^{iso} (ppm)	θ_{P-O-Al}
Al1	−4.0	6.6	0.66		P1	−14.3	134.9
Al2	23.2	7.4	0.84	0.86	P2	−15.4	139.5
Al3	24.8	4.6	0.82	0.47	P3	−7.7	127.9

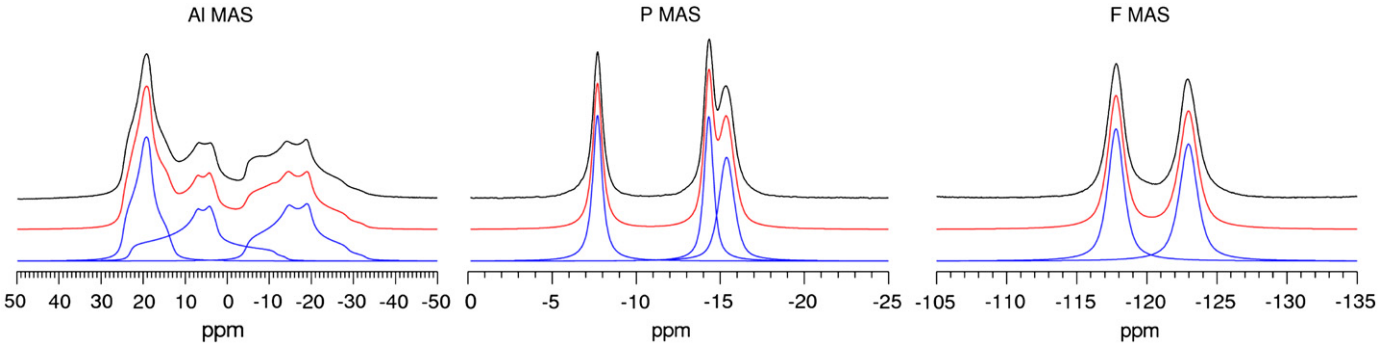

Fig. 4. ^{27}Al, ^{31}P and ^{19}F MAS NMR spectra of ULM-3 Al-MAPA. Experimental spectrum (top black line) is compared to model (middle red line) obtained as a sum of individual signals (bottom blue lines). (For interpretation of the references to colour in this figure legend, the reader is referred to the web version of this article.)

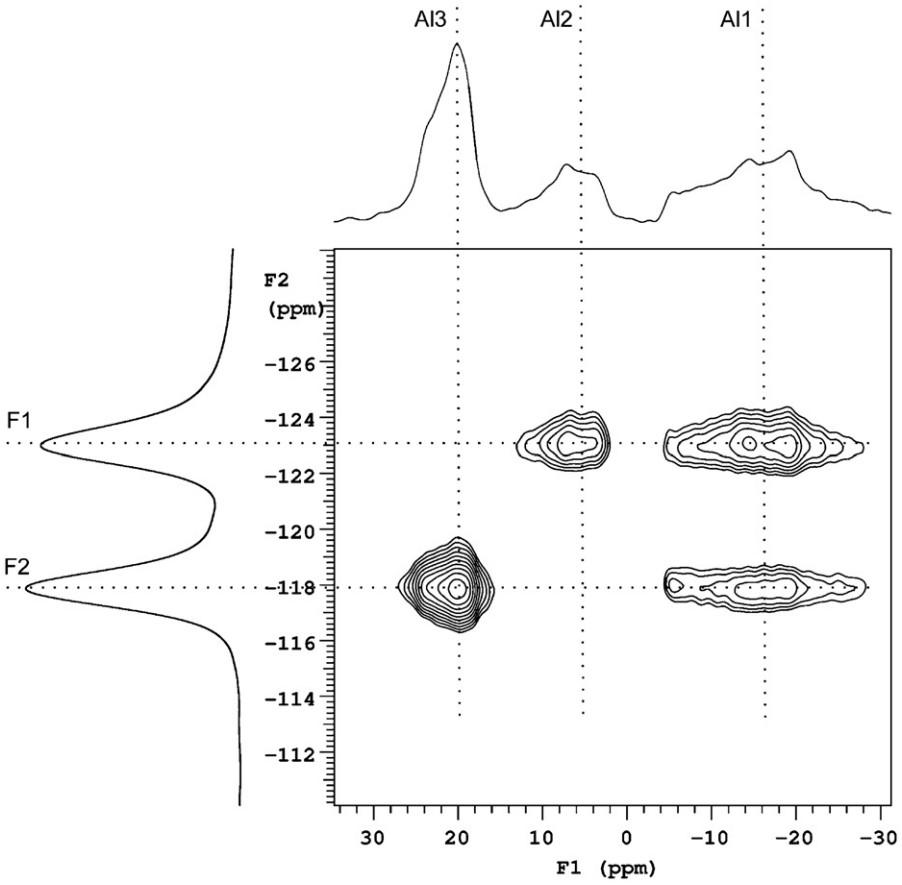

Fig. 5. Two-dimensional ^{27}Al–^{19}F HETCOR NMR spectrum of ULM-3 Al-MAPA, showing that both fluorine sites are bridging sites between a hexacoordinated aluminum and one of pentacoordinated aluminum sites. Based on an assigned aluminum spectrum and this two-dimensional spectrum one can assign fluorine signals to sites F1 and F2.

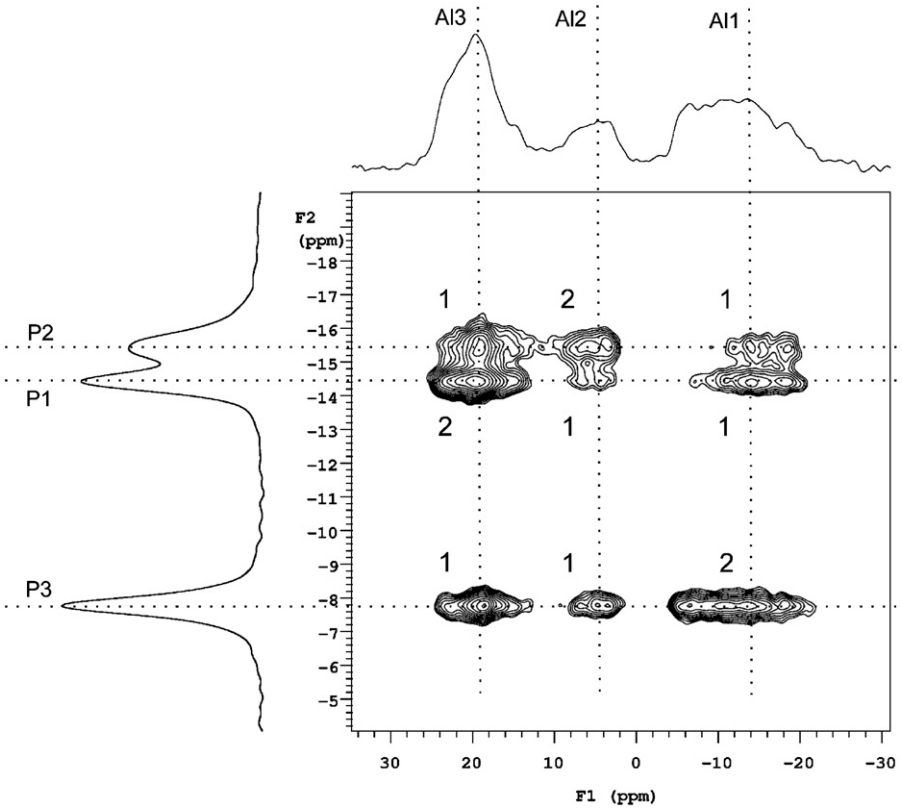

Fig. 6. Two-dimensional ^{27}Al–^{31}P HETCOR NMR spectrum of ULM-3 Al-MAPA, which allows one to deduce an Al–P connectivity table and thus to verify the assignment of phosphorus NMR signals to P1, P2 and P3 sites.

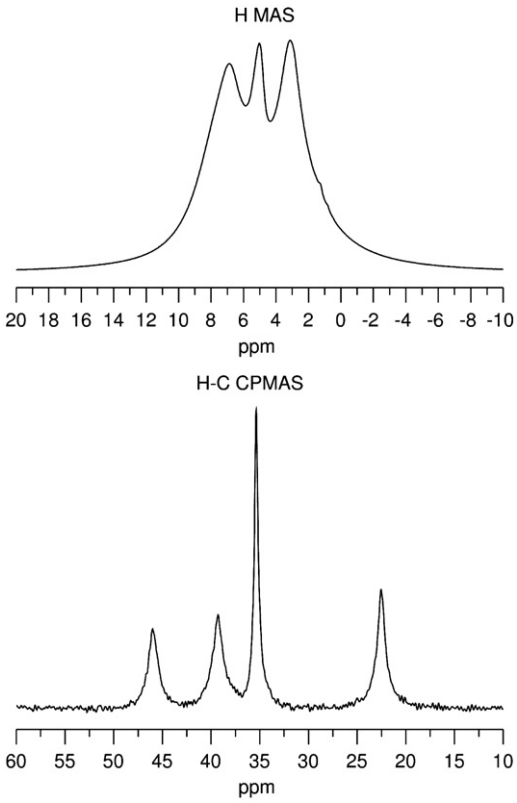

Fig. 7. ^{1}H MAS and ^{1}H–^{13}C CPMAS NMR spectra of ULM-3 Al-MAPA.

Table 7
Structural features of aluminophosphates/zinc phosphate with occluded 3-methylaminopropylamine species.

Structure	Dimensionality	Al/Zn coordination	P coordination	Framework (layer) charge	Protonation of MAPA	Reference
$AlPO_4$-21/ MDAP-2	3D	AlO_4, $AlO_4(OH)$, $AlO_4(OH)(OH_2)$	PO_4	Negative	Doubly protonated	[5,29]
Zinc phosphate	2D	ZnO_4	PO_4, HPO_4, H_2PO_4	Negative	Doubly protonated	[4]
MDAP-1	2D	AlO_4	PO_4	Negative	Doubly protonated	[29]
MDAP-3	2D	AlO_4	PO_4, HPO_4	Negative	Doubly protonated	[30]
ULM-3 Al-MAPA	3D	AlO_4F, AlO_4F_2	PO_4	Negative	Doubly protonated	Present work

resolve four signals belonging to four carbon atoms within the template molecule. None of the signals is split, showing that each carbon atom of the molecule occupies a single crystallographic site and which again confirms the selected crystallographic symmetry. Two possible positions for N2 atom are not reflected in the carbon spectrum. Obviously, local electronic environments of the neighboring carbon sites are not affected by the disorder. Among carbon signals, the one at 35.4 ppm is substantially narrower than the rest of the signals. It belongs to carbon in a terminal methyl group and it is probably narrower because the methyl group rotates around the C–N axis.

4. Conclusions

The use of 3-methylaminopropylamine in a fluoride medium leads to the formation of an aluminophosphate structure that is analogous to aluminophosphates ULM-4 Al and gallophosphate ULM-3, which were originally prepared in the presence of symmetric diamines. In a fluoride-free medium, 3-methylaminopropylamine favors the formation of $AlPO_4$-21 structure type. The examination of guest/host interactions in the structures that contain MAPA (Table 7) revealed that the position of MAPA in the structure and its interactions with the framework depended on the elemental composition of the inorganic framework (layers). The formed structures have no structural analogy, but the doubly protonated MAPA and the negatively charged frameworks, which suggest an important role of electrostatic interactions in the formation of the structures. In the case of ULM-3 Al-MAPA the asymmetry of MAPA does not affect the symmetry of the framework, whereas the 1,4-diaminobutane in ULM-3 Al lowers the structure symmetry due to the sub-network arrangement of the molecule.

Acknowledgments

The support by the Slovenian Ministry of Education, Science and Sport through the research program P1-0021-0104 and the Serbian Ministry of Science (the research project P-42055) is acknowledged.

References

[1] A.F. Ojo, L.B. McCusker, Zeolites 11 (1991) 460.
[2] A.K. Sinha, S. Sainkar, S. Sivasanker, Microporous Mesoporous Mater. 31 (1999) 321.

[3] N. Rajic, N. Zabukovec Logar, D. Stojakovic, S. Sajic, A. Golobic, V. Kaucic, J. Serb. Soc. 70 (2005) 625–633.
[4] N. Zabukovec Logar, N. Rajic, D. Stojakovic, S. Sajic, A. Golobic, V. Kaucic, Acta Cryst. E 61 (2005) m1354–m1356.
[5] D. Stojakovic, N. Rajic, N. Zabukovec Logar, S. Sajic, V. Kaucic, J. Therm. Anal. Cal. 87 (2007) 337–341.
[6] S. Oliver, A. Kuperman, A. Lough, G.A. Ozin, J. Mater. Chem. 7 (1997) 807–812.
[7] N. Rajic, A. Ristic, A. Tuel, V. Kaucic, Zeolites 18 (1997) 115–118.
[8] R.E. Morris, A. Burton, L.M. Bull, S.I. Zones, Chem. Mater. 16 (2004) 2844–2851.
[9] R. Garcia, I.J. Shannon, A.M.Z. Slawin, W. Zhou, P.A. Cox, P.A. Wright, Microporous Mesoporous Mater 58 (2003) 91–104.
[10] N. Simon, T. Loiseau, G. Ferey, J. Mater. Chem. 9 (1999) 585–589.
[11] M. Zhang, D. Zhou, J. Li, J. Yu, J. Xu, F. Deng, G. Li, R. Xu, Inorg. Chem. 46 (2007) 136–140.
[12] M. Wang, J.-Y. Li, Y. Li, X.-W. Song, J.-H. Yu, R.-R. Xu, Gaodeng Xuexiao Huaxue Xuebao (Chem. J. Chin. Univ.) 26 (2005) 1027–1029.
[13] P.S. Wheatley, C.J. Love, J.J. Morrison, I.J. Shannon, R.E. Morris, J. Mater. Chem. 12 (2002) 477–482.
[14] E.R. Cooper, C.D. Andrews, P.S. Wheatley, P.B. Webb, P. Wormald, R.E. Morris, Nature 430 (2004) 1012–1016.
[15] N. Simon, T. Loiseau, G. Ferey, J. Chem. Soc. Dalton Trans. (1999) 1147–1151.
[16] N. Simon, T. Loiseau, G. Ferey, Solid State Sci. 1 (1999) 339–349.
[17] N. Simon, N. Guillou, T. Loiseau, F. Taulelle, G. Ferey, J. Solid State Chem. 147 (1999) 92–98.
[18] W. Yan, J. Yu, Z. Shi, R. Xu, Inorg. Chem. 40 (2001) 379–383.
[19] E.R. Parnham, R.E. Morris, Chem. Mater. 18 (2006) 4882–4887.
[20] J.-L. Paillaud, C. Marichal, M. Roux, C. Baerlocher, J.M. Chezeau, J. Phys. Chem. B 109 (2005) 11893–11899.
[21] P.S. Wheatley, R.E. Morris, J. Solid State Chem. 167 (2002) 267–273.
[22] M.M. Harding, B.M. Kariuki, Acta Cryst. C 50 (1994) 852–854.
[23] W. Yan, J. Yu, Z. Shi, Y. Wang, Y. Zou, R. Xu, J. Solid State Chem. 161 (2001) 259–265.
[24] N. Simon, J. Marrot, T. Loiseau, G. Ferey, Solid State Sci. 8 (2006) 1361–1367.
[25] N. Zabukovec Logar, L. Golič, V. Kaučič, Microporous Mater. 9 (1997) 63–69.
[26] J. Renaudin, T. Loiseau, F. Taulelle, G. Ferey, C. R. Acad. Sci. Paris Ser. IIb 323 (1996) 545–553.
[27] T. Loiseau, R. Retoux, P. Lacorre, G. Férey, J. Solid State Chem. 111 (1994) 427–436.
[28] T. Loiseau, F. Taulelle, G. Férey, Microporous Mater. 5 (1996) 365–379.
[29] A. Tuel, J.-L. Jorda, V. Gramlich, C. Baerlocher, J. Solid State Chem. 178 (2005) 782–791.
[30] A. Tuel, Ch. Lorentz, V. Gramlich, C. Baerlocher, J. Solid State Chem. 178 (2005) 2322–2331.
[31] Crystallographica Search-Match, version 2,1,1,0, Oxford Cryosystems, UK, 2003.
[32] G.M. Sheldrick, SHELXL-97. Program for Crystal Structure Refinement, University of Göttingen, Germany, 1997.
[33] E. Dowty, Atoms v5.0, Shape Software, Kingsport, USA, 1999.
[34] L. Farrugia, Ortep3 for Windows v1.05, 1999.
[35] F. Taulelle, V. Munch, C. Huguenard, A. Samoson, T. Loiseau, N. Simon, J. Renaudin, G. Ferey, in: M.M.J. Treacy, B.K. Marcus, M.E. Bisher and J.B. Higgins, (Eds.), in: Proceedings of the 12th International Zeolite Conference, Baltimore, Maryland, USA, July 5–10, 1998. 4 (1999) 2409–2412.
[36] G. Engelhardt, W. Veeman, J. Chem. Soc. Chem. Commun. (1993) 622–623.
[37] D. Padro, A.P. Howes, M.E. Smith, R. Dupree, Solid State Nucl. Magn. Reson. 15 (2000) 231–236.
[38] D. Müller, E. Jahn, G. Ladwig, U. Haubenreisser, Chem. Phys. Lett. 109 (1984) 332–336.
[39] C.A. Fyfe, H. Meyer zu Altenschildesche, K.C. Wong-Moon, H. Grondey, J.M. Chazeau, Solid State Nucl. Magn. Reson. 9 (1997) 97–106.
[40] D. Massiot, F. Fayon, M. Capron, I. King, S. Le Calvé, B. Alonso, J.-O. Durand, B. Bujoli, Z. Gan, G. Hoatson, Magn. Reson. Chem. 40 (2002) 70–76.